

CHROM. 15,481

COMPLEX-FORMING EQUILIBRIA IN ISOTACHOPHORESIS

III. ESTIMATION OF OPTIMUM SEPARATION CONDITIONS OF SEVERAL ORGANIC ACIDS BY MEANS OF COMPUTER SIMULATION

TAKESHI HIROKAWA* and YOSHIYUKI KISO

Applied Physics and Chemistry, Faculty of Engineering, Hiroshima University, Shitami, Saijo Higashi-hiroshima 724 (Japan)

(Received October 29th, 1982)

SUMMARY

A computer simulation of isotachophoretic equilibria utilizing a complex-forming technique was applied for the estimation of optimum separation conditions for several previously studied organic acids. The simulations confirmed that the electrolyte system which had been employed was optimal for these separations. Good agreement was obtained between the observed and the simulated isotachopherograms and the injected sample amounts could be estimated, confirming the practical applicability of this simulational technique to analytical problems.

INTRODUCTION

The separability of mixtures by isotachophoresis has been improved using several techniques, such as adjustment of the pH of a leading electrolyte, the use of a complex-forming counter ion and the use of a mixed solvent for electrolyte systems. These techniques are intended to cause differences among the effective mobilities of the components sufficient for their separation. As described in Part I¹, isotachophoresis has a unique feature in that the effective mobilities and the concentrations of sample components in separated zones can be simulated with the aid of a computer. These simulations may be utilized for analytical purposes, such as an assessment of the separability of mixtures under electrolyte conditions and the prediction of time-based zone length for a certain amount of sample. Possible applications are the evaluation of the absolute mobilities and pK_a values of ionic substances and of the stability constants of complexes, as described in Part II².

The complex-forming technique has proved to be a powerful one for the separation of ions with similar effective mobilities in a normal electrolyte system which utilizes the pH dependence of effective mobility. However, the success of such separations depends on the complexing agent used, its concentration, the pH of the leading electrolyte and the concentration of the leading ion. Therefore, the choice of optimum electrolyte system may sometimes be difficult without any theoretical prediction, and as a result few applications have been reported.

To test the analytical utility of computer simulation for the establishment of optimum separation conditions, we have simulated complex-forming equilibria for several organic acids investigated by Kaniansky and Everaerts³, and compared the obtained isotachopherograms with the observed ones.

SIMULATION CONDITIONS

The samples were those employed in ref. 3, perchlorate, formate (For), tartrate (Tar), citrate (Cit), α -ketoglutarate (α -Ket), acetate (Ac), lactate (Lac), 2-hydroxybutyrate (2HB) and caproate (Cap) ions, and the previous experimental conditions and results were used in the presents simulation. The samples are weak acids except for perchloric acid. Three kinds of interacting counter ions, Ca^{2+} , Cd^{2+} and Al^{3+} , were examined individually, by adding a few mM of their chlorides to leading electrolytes. The leading and terminating ions were chloride (10 mM) and 2-N-morpholinoethanesulphonate (MES), respectively. The pH of the leading electrolyte, pH_L , was adjusted

TABLE I

PHYSICO-CHEMICAL CONSTANTS USED IN SIMULATION (25°C)

m_0 = Absolute mobility ($\text{cm}^2 \text{V}^{-1} \text{sec}^{-1}$) $\times 10^5$; $\text{p}K_a$ = thermodynamic acidity constant, assumed values being used for Cl^- and ClO_4^- ; $\log K$ = thermodynamic stability constant of calcium complex. The mobilities of complexes without asterisks were assumed using $m = (329.9/\sqrt{\text{formula weight} - 1.1}) \times 10^{-5} \text{ cm}^2 \text{V}^{-1} \text{sec}^{-1}$. The other constants were evaluated⁴ by analysing the relative step heights observed by Everaerts and co-workers⁵. The stability constants of the citrate and tartrate complexes used are slightly different from those in Part II, due to the slight difference in absolute mobility of citrate and tartrate ions.

Sample	m_0	$\text{p}K_a$	Complex	
			m_0	$\log K$
Cl	79.08*	-3		
ClO_4	69.8*	-2		
For	57.1	3.796		
Tar	34.6	3.036*	22.9	1.59*
	60.5	4.366*	0	2.879**
Cit	31.0	3.128*	22.2**	1.15*
	53.4	4.761*	0	2.897**
	70.8	6.396*	22.2**	4.788**
α -Ket	37.5	2.800	-	-
	59.0	5.272	0	2.26*
Ac	42.4*	4.756*	32.0	1.16**
Lac	36.5*	3.858*	28.0	1.34**
2HB	33.5**	3.98*	26.5	1.5**
Cap	30.2**	4.857*	-	-
MES	28.3**	6.095*	-	-
<i>Buffer</i>				
β -Ala	31.0**	3.55*		
ϵ -AMC	28.8**	4.43*		
His	29.6**	6.04*		
Tris	29.5**	8.067*		

* Literature value.

** Constant evaluated isotachophoretically in our laboratory.

to 6 by adding histidine. In the present simulations the electrolyte system contained Ca^{2+} .

The physico-chemical constants used in the simulations are listed in Table I. Since the absolute mobility of several samples were not available from the previous works, ones isotachophoretically evaluated⁴ by analysing the relative step heights of Everaerts *et al.*⁵ were used. The stability constants of calcium tartrate and calcium citrate complexes were slightly different from those in Part II², due to a re-evaluation using different ligand mobilities. Other values were taken from the literatures⁶⁻⁹. For the stability constant of the complex between 2-hydroxybutyrate and Ca^{2+} , an approximate value was estimated so as to reproduce an observed qualitative index. The absolute mobilities of complex ions especially kinetically labile ones, are not generally available from the literature. Therefore, it was assumed that the mobility varies inversely as the square root of the formula weight. The relation

$$m_0 = (329.9/\sqrt{\text{FW}} - 1.1) \times 10^{-5} \text{ cm}^2 \text{ V}^{-1} \text{ sec}^{-1} \quad (1)$$

is valid for carboxylate ions of the type $n\text{-C}_n\text{H}_{2n+1}\text{COO}^-$ where $n = 1-7$.

For the simulations, a Sord microcomputer M223 Mk III was used. Figures including simulated isotachopherograms were plotted using a Watanabe x - y plotter Model WX4671, which was controlled by the computer.

Isotachopherograms were simulated as follows. First, the R_E values and the time-based zone length were evaluated. The R_E values control the step heights of signals, which can be obtained by a conductometric or a potential gradient detector. The ascending profiles of steps were simulated using hyperbolic tangent (tanh) functions. The step widths are proportional to the time-based zone lengths. The differential signals of the steps were simulated using asymmetric Gaussians, and the peak heights are proportional to the difference between adjacent R_E values.

RESULTS AND DISCUSSION

First, the possibility of separation was investigated for electrolyte systems utilizing the pH dependence of the effective mobility. Fig. 1 shows the pH dependences of the effective mobilities of the samples. Among them, tartrate and α -ketoglutarate can be dianions, and citrate can be a trianion in the high pH range. The others are monoanions. The curves in Fig. 1 are not for the isotachophoretically steady state but for infinitely diluted electrolyte solutions, and were plotted by use of the absolute mobilities and thermodynamic dissociation constants in Table I. The pH in Fig. 1 is that of the sample zones, pH_s . The effective mobilities of isotachophoretically separated samples are different from those in Fig. 1, since the zones have finite ionic strength and the mobility varies according to its magnitude. The order of detection expected from Fig. 1, namely the order of magnitude of the effective mobility, may be different from the real order of detection, since mobility decreases with increasing charge number on the ions. In spite of this, Fig. 1 can be used for a rough estimation of the separation conditions. Since the curves for several samples in Fig. 1 are close together and intersect with each other, a good separation would seem to be difficult. For an exact assessment of separability, a simulational calculation for an isotachophoretically steady state is necessary. In the separated zones, not only the ionic

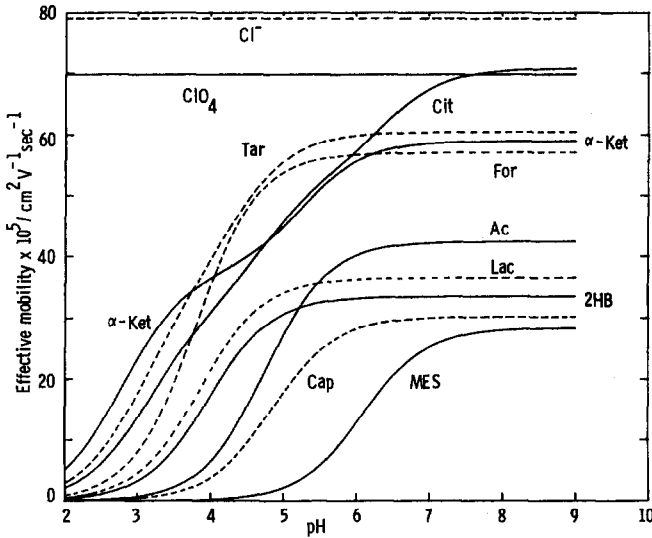


Fig. 1. Effect of pH on the effective mobility of the samples. The absolute mobilities and thermodynamic dissociation constants listed in Table I were used. Samples: chloride (Cl); perchlorate (ClO_4); formate (For); tartrate (Tar); citrate (Cit); α -ketoglutarate (α -Ket); acetate (Ac); lactate (Lac); 2-hydroxybutyrate (2HB); caproate (Cap); N-morpholinoethanesulphonate (MES). The curves are not for the isotachophoretically steady state and ionic strength is zero.

strength but also the pH_S values are different from each other. In anionic analysis, the pH_S values are generally higher than the pH_L .

The differences in R_E , *i.e.*, the proposed qualitative index, among the samples can be used for assessment of the separability. The index is equal to the ratio of step heights, h , of potential gradients, E , of specific conductivities, κ , and of effective mobilities, \bar{m} , as follows

$$R_E = h_s/h_L = E_s/E_L = \kappa_L/\kappa_S = \bar{m}_L/\bar{m}_S \quad (2)$$

where subscripts L and S denote the leading and the sample zones or ions. According to our practical experience, when the difference between the R_E values of two samples at the steady state is within *ca.* 0.15, the separation of the samples may be difficult or sometimes time-consuming, since a high load of leading ion or a longer separation tube is necessary.

The leading electrolytes used in simulations were 10 mM hydrochloric acid buffered by β -alanine (β -Ala), ϵ -aminocaproic acid (ϵ -AMC), histidine (His), and tris(hydroxymethyl)aminomethane (Tris), which have been used conveniently in practical analyses. The pH of the leading electrolytes, pH_L , was varied in the range of 2.7–4.2 by β -ala, 3.8–5.4 by ϵ -AMC, 5–7 by His and 6.9–9 by Tris. The R_E values of nine anions and a terminating ion (MES) were simulated for each 0.1 pH in the above pH_L range. Fig. 2 shows the effect of pH_L on the R_E values. The curves intersect with each other at several pH_L . In the pH_L range of 6–9, citrate, formate, tartrate and α -ketoglutarate ions may be difficult to separate. The separation of formate and tartrate may be especially difficult throughout the pH_L range considered. In the lower

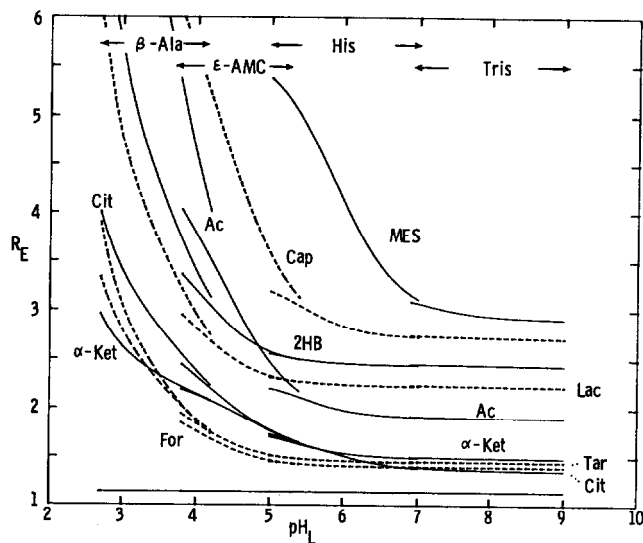


Fig. 2. Effect of pH_L and the buffers on the simulated R_E values of the samples at the isotachophoretically steady state. The leading ion was 10 mM Cl^- . The buffers used were β -alanine (β -Ala; $\text{pH}_L = 2.7 - 4.2$), ϵ -aminocaproic acid (ϵ -AMC; $3.8 - 5.4$), histidine (His; $5 - 7$) and tris(hydroxymethyl)aminomethane (Tris; $6.9 - 9$). Ca^{2+} was not contained in the leading electrolyte. For samples, see Fig. 1.

pH_L range of $4.5 - 6$, the separation of citrate and α -ketoglutarate may also be difficult. In the pH_L range, acetate ion may form a mixed zone with lactate and 2-hydroxybutyrate ions. Thus, sufficient separation could not be expected under electrolyte conditions utilizing the pH dependence of the effective mobility. The pH dependences of the effective mobilities of the samples are shown in Fig. 3. There is a distinct

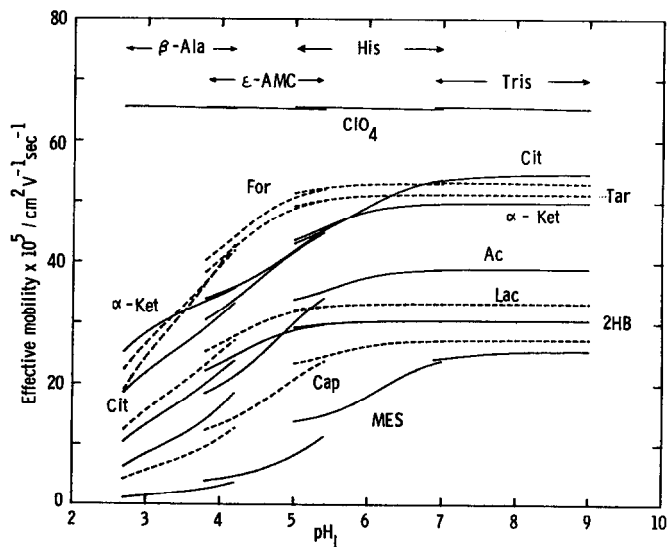


Fig. 3. Effect of pH_L and the buffers on the simulated effective mobilities of the samples at the isotachophoretically steady state. For the electrolyte systems, see Fig. 2.

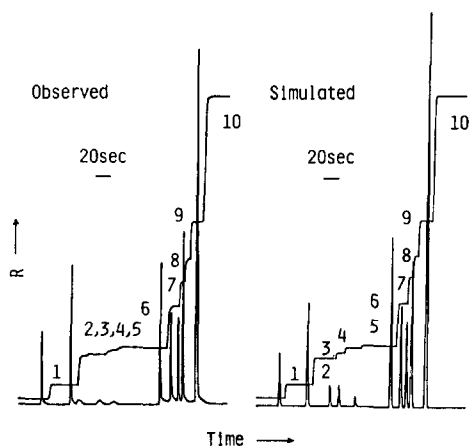


Fig. 4. Observed isotachopherogram at $\text{pH}_L = 6$ from ref. 3 and the simulated one. Samples: perchlorate (1); formate (2); tartrate (3); citrate (4); α -ketoglutarate (5); acetate (6); lactate (7); 2-hydroxybutyrate (8); caproate (9). The terminating ion (10) was N-morpholinoethanesulphonate. Samples 2-5 formed a mixed zone in the observed isotachopherogram.

difference between Figs. 1 and 3, due to the finite ionic strength in the sample zones; the order of the effective mobility in the high pH_L range is different. Owing to the pH shift of the sample zones, the anions are more mobile in the low pH_L range than expected from Fig. 1.

Under the experimental conditions used in ref. 3 ($\text{pH}_L = 6$, histidine buffer), a mixed zone between formate, tartrate, citrate and α -ketoglutarate has been observed, in agreement with the present simulations. Fig. 4 shows the good agreement between

TABLE II

OBSERVED AND SIMULATED R_E VALUES OF THE SAMPLES, EFFECTIVE MOBILITIES AND CONCENTRATIONS OF ZONE CONSTITUENTS (25°C)

R_E = Ratio of potential gradients, E_s/E_L ; \bar{m}_s = effective mobility ($\text{cm}^2 \text{V}^{-1} \text{sec}^{-1}$) of sample ion, $\times 10^5$; pH_s = pH of sample zone; \bar{Z} = apparent charge of sample; C^t = total concentration (mM) of sample; $C_{B,S}^t$ = total concentration (mM) of buffer (histidine); $\bar{m}_{B,S}$ = effective mobility ($\text{cm}^2 \text{V}^{-1} \text{sec}^{-1}$) of buffer ion, $\times 10^5$; I = ionic strength $\times 10^3$.

Sample	R_E		\bar{m}_s	pH_s	\bar{Z}	C^t	$C_{B,S}^t$	$\bar{m}_{B,S}$	I
	Obs.	Calc.							
ClO_4	1.16	1.14	65.5	6.015	-1.00	9.649	17.87	-14.2	9.65
For	(1.43)	1.41	53.0	6.046	-0.99	9.040	17.26	-13.7	8.99
Tar	-	1.46	51.1	6.055	-1.99	4.517	17.22	-13.4	13.4
Cit	-	1.51	49.3	6.081	-2.45	3.567	17.21	-13.0	15.6
α -Ket	(1.53)	1.54	48.4	6.072	-1.90	4.594	17.09	-13.2	12.9
Ac	Std.*	1.98	37.6	6.122	-0.96	8.048	16.27	-12.7	7.74
Lac	2.24	2.24	33.2	6.122	-1.00	7.520	15.74	-12.7	7.48
2HB	2.47	2.46	30.3	6.141	-0.99	7.211	15.43	-12.4	7.17
Cap	2.89	2.84	26.3	6.190	-0.96	6.832	15.05	-11.7	6.55
MES	4.24	4.13	18.0	6.421	-0.69	6.597	14.82	- 8.42	4.58

* Internal standard.

a reverse trace (*i.e.*, with time increasing in the opposite direction) of the observed isotachopherogram³ and the simulated one. It should be noted that the present simulation did not consider a transient state or mixed zone formation, therefore the simulated zone boundaries between formate, tartrate, citrate and α -ketoglutarate are clear and the differential curves corresponding to the boundaries are sharper and stronger in comparison with the observed ones. In the mixture, the difference between the simulated R_E values of formate (No. 2 in Fig. 4) and α -ketoglutarate (No. 5) was 0.13.

In ref. 3, the injected sample amounts were not cited, therefore the amounts were estimated by simulation, as discussed in a later section. Table II shows the R_E values estimated from the original isotachopherograms³ and the simulated values, the effective mobilities and the concentrations of the zone constituents. The observed step heights of the samples were converted into R_E values using the simulated R_E value of acetic acid as an internal standard⁴. The exact step heights of tartrate and citrate ions could not be determined due to the mixed zone. The R_E values of formate and tartrate were estimated from the initial and the final parts of the continuous mixed zone.

For separation, the R_E values or the effective mobility must be varied among the samples using a different technique. Those of formate and tartrate ions are accidentally very close in the pH_L range 3–9, although the first is a monoanion and the second can be a dianion. To separate the samples, Kaniansky and Everaerts used a leading electrolyte buffered by histidine ($\text{pH}_L = 6$) which contained 2 mM Ca^{2+} . The Ca^{2+} migrates into the sample zones forming kinetically labile complexes. For example, the complex-forming equilibria of tartrate ion can be written



where K_1 and K_2 are the dissociation constants of tartaric acid, and K_3 and K_4 are the stability constants of CaHTar^+ and CaTar complexes. Through the formation of the CaTar complex with null electric charge and CaHTar^+ with a positive charge, the decrease in effective mobility and increase in R_E value can easily be estimated¹. The R_E value of tartrate ion can be expressed as

$$\begin{aligned}
 R_E(\text{Tar}) &= \bar{m}_{\text{Cl}}/\bar{m}_{\text{Tar}} \\
 &= \frac{\bar{m}_{\text{Cl}} ([\text{H}_2\text{Tar}] + [\text{HTar}^-] + [\text{Tar}^{2-}] + [\text{CaHTar}^+] + [\text{CaTar}])}{m_1 [\text{HTar}^-] + m_2 [\text{Tar}^{2-}] + m_3 [\text{CaHTar}^+]} \\
 &= \frac{\bar{m}_{\text{Cl}} \{1 + K_1/[\text{H}^+](1 + K_3 [\text{Ca}^{2+}]) + K_1 K_2/[\text{H}^+]^2(1 + K_4 [\text{Ca}^{2+}])\}}{K_1/[\text{H}^+](m_1 + m_3 [\text{Ca}^{2+}]) + m_2 K_1 K_2/[\text{H}^+]^2}
 \end{aligned}
 \tag{4}$$

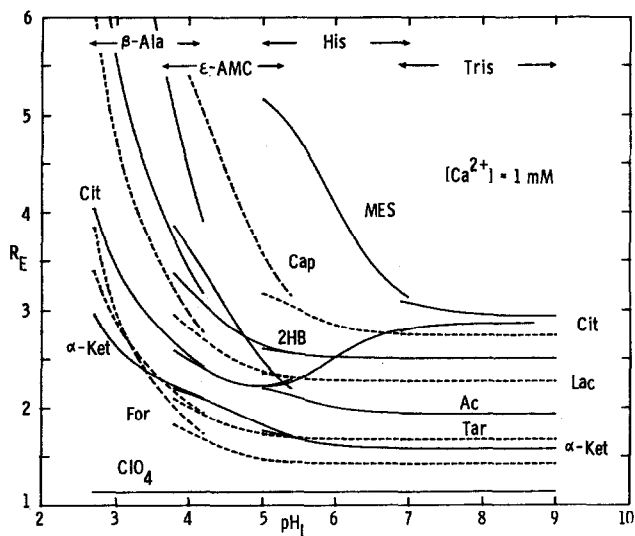


Fig. 5. Effect of pH_L and buffers on the simulated R_E values of the samples. The leading electrolyte contained 1 mM Ca^{2+} . For samples, see Fig. 1.

where m_1 is the mobility of HTar^- corrected to finite ionic strength, m_2 that of Tar^{2-} and m_3 that of the CaHTar^+ complex. From eqn. 4, above the medium pH range, the R_E value may be larger than that of formate due to the smaller stability constant of calcium formate, suggesting the possibility of separation between them. Similar complex formation and a similar difference in R_E values compared to an electrolyte system without Ca^{2+} ions can be expected for the other samples, except for perchlorate, caproate and MES ions, of which the complex stability constants might be very small. If the abundances of the calcium complexes, which are strongly influenced by the concentration of Ca^{2+} in the leading electrolyte and the pH_L , are sufficiently large they can be separated.

The complex-forming equilibria were simulated, varying the concentration of Ca^{2+} in the range of 1 – 3 mM. Although Kaniansky and Everaerts fixed the pH_L at 6, in our simulations the effect of pH_L on the isotachophoretic equilibria was also investigated in the pH_L range of 2.7–9. The pH buffers used were the same as with the above electrolyte systems. By adding Ca^{2+} to the leading electrolyte, a significant decrease in the effective mobility was expected for the strongly interacting tartrate, α -ketoglutarate and citrate ions. Fig. 5 shows the simulated R_E values using a leading electrolyte containing 1 mM Ca^{2+} . In comparison with Fig. 2, by adding such a small amount of Ca^{2+} , the remarkable variation of R_E can be simulated. The adjacent curves of formate, tartrate, citrate and α -ketoglutarate above the medium pH_L range in Fig. 2 were resolved in Fig. 5. The differences in R_E values among the samples may be satisfactory for separation in the limited pH_L range of 3.8–4.2, buffered by ϵ -AMC. The separation in this pH_L range is due to both the complex-forming effect and the increased pH shift upon adding Ca^{2+} ion.

A higher pH_L of ca. 6.2 and a pH_L range of 7.2–7.5 may be reasonably good electrolyte conditions, although the difference in R_E values might be too small for

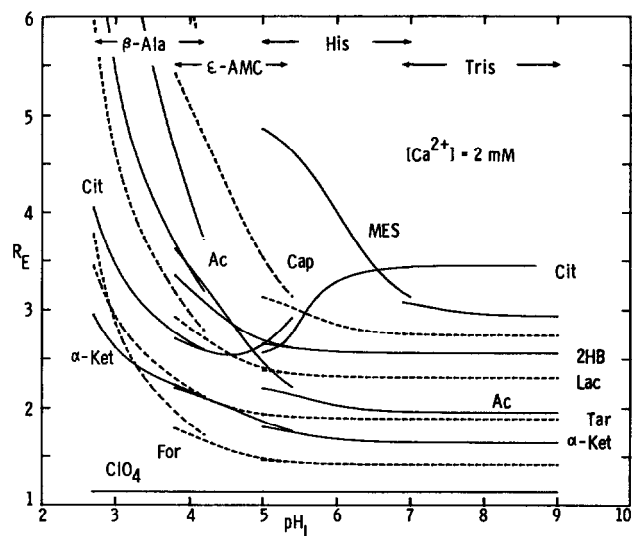


Fig. 6. Effect of pH_L and buffers on the simulated R_E values of the samples. The leading electrolyte contained 2 mM Ca^{2+} . Kaniansky and Everaerts³ selected pH_L 6 for separation.

complete separation. Fig. 6 shows the effect of pH_L on the R_E values in an electrolyte system containing 2 mM Ca^{2+} . Apparently, the pH_L range of *ca.* 5.8–6.2 is suitable for separation. The electrolyte condition used previously³ was just in this range. If the selection of pH_L had not been appropriate the samples could not have been separated. The higher pH_L range may also be useful. However, a different terminating ion is necessary, for example, N-tris(hydroxymethyl)methyl-3-aminopropanesulphonic acid (TAPS), since the complexing citrate ion cannot be detected in the presence of the

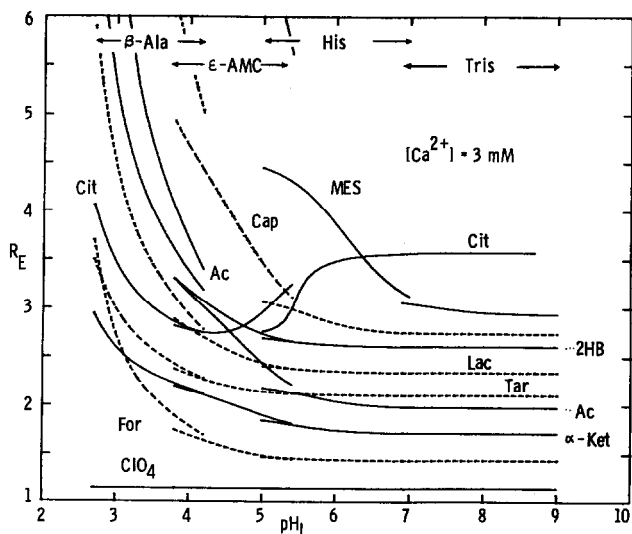


Fig. 7. Effect of pH_L and buffers on the simulated R_E values of the samples. The leading electrolyte contained 3 mM Ca^{2+} .

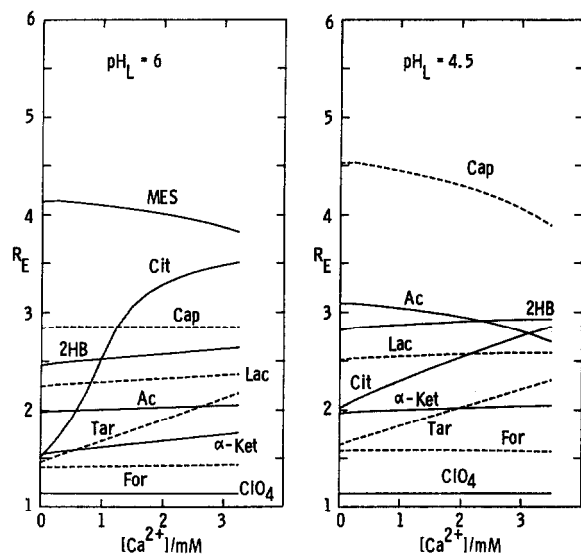


Fig. 8. Effect of the concentration of Ca^{2+} in the leading electrolyte on the R_E values at pH_L 6 (buffer: His) and 4.5 (*e*-AMC). The leading ion was 10 mM Cl^- .

terminating ion MES. In the low pH_L range of 3.8–5, the separation of tartrate, α -ketoglutarate, citrate and lactate may be difficult. Fig. 7 shows the effect of pH_L on the R_E values in an electrolyte system containing 3 mM Ca^{2+} . Separation may be achieved in the high pH_L range using the different terminating ion. The order of the R_E values of tartrate and acetate was reversed, due to the strong complex-forming effect of tartrate, in comparison with Fig. 6. The samples may also be separated in the low pH_L range of 3.3–3.8. However, the R_E values of caproate ion and especially MES become larger, and in practice MES may not be suitable as the terminating ion in this pH_L range. Fig. 8 summarizes the effect of the concentration of Ca^{2+} in the leading electrolyte on the simulated R_E values at pH_L 6 and 4.5. The increases in R_E values are due to complex formation and the decrease for the weakly interacting samples are

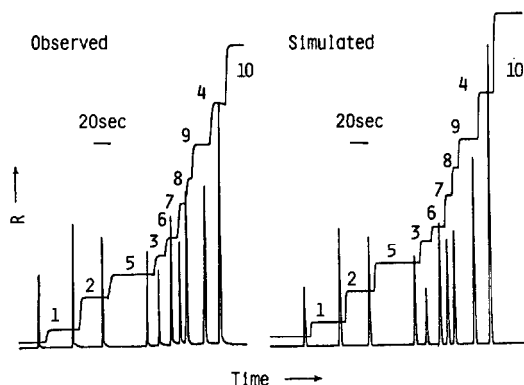


Fig. 9. Observed isotachopherogram at $\text{pH}_L = 6$ from ref. 4 and the simulated one. The leading electrolyte contained 2 mM Ca^{2+} . Samples as in Fig. 4. The separation was complete.

TABLE III

OBSERVED AND SIMULATED R_E VALUES OF THE COMPLEX-FORMING SAMPLES, EFFECTIVE MOBILITIES AND CONCENTRATIONS OF ZONE CONSTITUENTS (25°C)

C'_S = Total concentration (mM) of uncomplexed sample; $C'_{M,S}$ = Total concentration (mM) of uncomplexed Ca^{2+} ;
 $\bar{m}_{M,S}$ = Effective mobility ($cm^2 V^{-1} sec^{-1}$) of Ca^{2+} , $\times 10^5$; for other notations, see Table II.

Sample	R_E		\bar{m}_S	pH_S	Z	C'	C'_S	$C'_{M,S}$	\bar{m}_M	$C'_{B,S}$	$\bar{m}_{B,S}$	I
	Obs.	Calc.										
ClO_4	1.13	1.14	65.6	6.015	-1.00	9.566	-	1.89	-53.9	10.7	-14.1	11.5
For	1.45	1.42	52.4	6.050	-0.98	8.817	8.76	1.65	-53.3	13.6	-14.1	10.4
Tar	1.84	1.90	39.3	6.091	-1.51	4.536	3.45	1.00	-25.7	9.76	-13.0	11.2
Cit	3.33	3.29	22.7	6.169	-1.14	4.735	0.52	0.80	7.12	8.49	-12.0	7.23
α -Ket	1.65	1.68	44.4	6.085	-1.74	4.500	4.12	1.39	-41.8	10.0	-13.0	12.9
Ac	Std.*	2.03	36.8	6.138	-0.94	7.643	7.55	1.32	-52.9	9.71	-12.4	8.59
Lac	2.34	2.32	32.1	6.129	-0.96	7.075	6.95	1.19	-51.9	9.33	-12.5	8.11
2HB	2.59	2.57	29.0	6.150	-0.95	6.732	6.57	1.09	-51.0	9.13	-12.2	7.62
Cap	2.88	2.85	26.2	6.201	-0.96	6.351	-	1.11	-55.1	9.02	-11.5	7.21
MES	3.90	4.01	18.6	6.474	-0.72	6.003	-	0.86	-55.9	6.00	-7.70	5.19

* Internal standard.

due to the increased pH shift caused by the addition of Ca^{2+} . The decreases are apparent for MES at pH_L 6 and acetic and caproic acid at pH_L 4.5, their pK_a values being close to the pH_L .

Thus, when MES is used as the terminating ion, it is apparent that the leading electrolyte containing 2 mM Ca^{2+} buffered by histidine ($pH_L = 6$) is optimum for separation of these samples. Fig. 9 shows the satisfactory agreement between a reverse trace of the observed isotachopherogram³ and the simulated one under the same conditions. The injected amount was the same as those in Fig. 4, but the time scales are a little different in the two Figures. Table III lists the observed and simulated R_E values, effective mobilities and concentrations of the zone constituents.

TABLE IV

MEASURED ZONE-PASSING TIMES* AND EVALUATED AMOUNTS** OF IONS

Sample	$[Ca^{2+}] = 2 mM$		$[Ca^{2+}] = 0 mM$	
	Time (sec)	Amount (nmol)	Time (sec)	Amount (nmol)
ClO_4	40.9	27	37.5	28
For	33.8	21		
Tar	13.3	4.2		
Cit	18.7	6.1		
α -Ket	53.3	16.6		
Ac	15.6	8.3	13.5	8.3
Lac	8.9	4.4	9.0	5.2
2HB	8.0	3.7	6.0	3.3
Cap	23.1	10	20.0	11

* Measured from the original figures in ref. 3.

** The driving current was assumed to be 100 μA .

Estimation of sample amounts

In ref. 3 the injected sample amounts were not cited, except for the volume (1 μl). Thus, the amounts were estimated from the given isotachopherograms. For this purpose the value of the applied current is necessary. Although a current density (J) of 0.05 A cm^{-2} was cited, the internal cross-section of the detector used was not³. We assumed a driving current of $100 \mu\text{A}$, since the calculated inner diameter from the current density was 0.5 mm , which was very probable. First, the time of passage of the samples through a detector was estimated from the original figure³ for an electrolyte system containing 2 mM Ca^{2+} , since all of the samples were separated. These times are listed in Table IV, and correspond to the zone lengths divided by the isotachopheretic velocity, $v(\text{cm/sec})$. The injected sample amount, $n(\text{mol})$, is equal to the sample amount in the zone volume, namely, the concentration of sample multiplied by the volume. It should be noted that this concentration is different from that of the injected sample, since it is controlled by Kohlrausch's regulating function in the isotachopheretically steady state. Thus, the following equation was used to evaluate n

$$n = 1000 C^t \pi r^2 vt = 1000 C^t \pi r^2 E_L \bar{m}_L t = 1000 C^t \bar{m}_L I t / \kappa_L \quad (5)$$

where C^t is the total concentration (mol/l) of sample including the formed complexes, \bar{m}_L ($\text{cm}^2 \text{ V}^{-1} \text{ sec}^{-1}$) the effective mobility of leading ion, I the driving current (A), r (cm) the inner radius of separating tube, t (sec) the passage time and κ_L (S cm^{-1}) the specific conductivity of the leading zone. The \bar{m}_L and κ_L can be replaced by the corresponding amounts in the sample zone, since $\bar{m}_L E_L = \bar{m}_S J / \kappa_S$ is the isotachopheretic velocity which at the steady state is equal to $\bar{m}_S J / \kappa_S$. The simulated values of C^t are listed in Table III. The temperature of the separation and detection compartments was assumed to be 25°C . The effective mobility of the leading ion, Cl^- , was

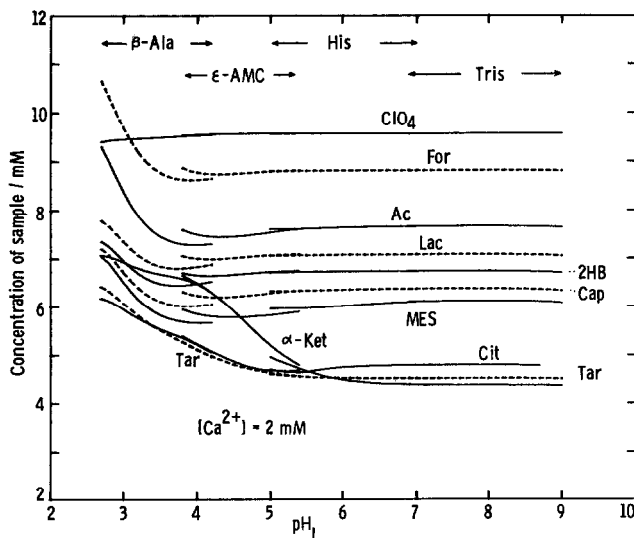


Fig. 10. Effect of pH_L and buffers on the simulated concentration of the samples at the isotachopheretically steady state. The leading electrolyte contained 2 mM Ca^{2+} . For samples, see Fig. 1.

$74.61 \cdot 10^{-5} \text{ cm}^2 \text{ V}^{-1} \text{ sec}^{-1}$, the specific conductivity of the leading zone was $1.0776 \text{ mS cm}^{-1}$ and the driving current was $100 \mu\text{A}$. Inserting these values into eqn. 5 gave the separated sample amounts shown in Table IV. The isotachophoretic velocity was $3.526 \cdot 10^{-2} \text{ cm sec}^{-1}$. For the simulation of the isotachopherograms in Figs. 4 and 9, the sample amounts evaluated by the above analysis were used.

Sample amounts for the non-complexing electrolyte system were estimated similarly. The simulated values of C_S^1 for the samples are shown in Table III. The effective mobility of the leading ion, Cl^- , was $74.53 \cdot 10^{-5} \text{ cm}^2 \text{ V}^{-1} \text{ sec}^{-1}$ and the specific conductivity of the leading zone was $0.97211 \text{ mS cm}^{-1}$ at 25°C . The evaluated sample amounts are listed in Table IV. A good agreement was obtained between the injected amounts of both electrolyte systems, as expected from the fact that the same volume of sample ($1 \mu\text{l}$) was injected. The amounts of formate, tartrate, citrate and α -ketoglutarate could not be compared due to formation of a mixed zone. The evaluated isotachophoretic velocity was $3.904 \cdot 10^{-2} \text{ cm sec}^{-1}$.

It should be noted that the total concentrations of the samples in both electrolyte systems were different. Figs. 10 and 11 show the effects of pH_L and buffers and the total concentrations of the samples. Apparently, the addition of Ca^{2+} lowers the sample concentration, even if a complex is not formed, for example, caproate.

Thus, the present computer simulations have revealed that such simulations can be utilized not only for the evaluation of physico-chemical constants of sample ions but also for the assessment of separation and analytical problems. A brief theoretical treatment concerning to quantitation will be reported elsewhere, together with its applications¹⁰.

In our laboratory, physico-chemical constants (absolute mobilities and $\text{p}K_a$ values) of a few hundred anions and cations are stored in a disk-based data file (data-bank) of a microcomputer, and using this the construction of a computer system for

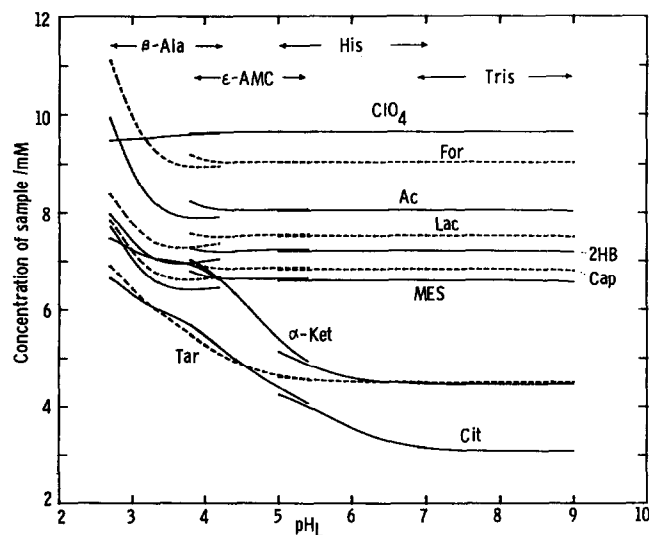


Fig. 11. Effect of pH_L and buffers on the simulated concentration of the samples at the isotachophoretically steady state. The leading electrolyte did not contain Ca^{2+} .

ready simulation is now in progress. The computer system can be applied to analytical problems and to the evaluation of mobilities, pK_a values, and stability constants of complexes. Moreover, qualitative and quantitative analysis may be possible by analysing observed isotachopherograms, if the R_E values and the time-based zone lengths can be measured exactly.

REFERENCES

- 1 T. Hirokawa and Y. Kiso, *J. Chromatogr.*, 242 (1982) 227.
- 2 T. Hirokawa and Y. Kiso, *J. Chromatogr.*, 248 (1982) 341.
- 3 D. Kaniansky and F. M. Everaerts, *J. Chromatogr.*, 148 (1978) 441.
- 4 T. Hirokawa, M. Nishino and Y. Kiso, *J. Chromatogr.*, 252 (1982) 49.
- 5 F. M. Everaerts, J. L. Beckers and Th. P. E. M. Verheggen, *Isotachophoresis*, Elsevier, Amsterdam, 1976.
- 6 R. A. Robinson and R. H. Stokes, *Electrolyte Solutions*, Butterworths, London, 2nd ed., 1959.
- 7 *Landolt-Börnstein, Zahlenwerte und Funktionen*, 6 Aufl. Bd. II, Teil 7, Springer, Berlin, 1960.
- 8 *Stability Constants of Metal-Ion Complexes*, L. G. Sillen and A. E. Martell (Editors), Special publication No. 17. The Chemical Society, London, 1964.
- 9 *International Critical Tables of Numerical Data, Physics, Chemistry and Technology*, Vol. VI, McGraw-Hill, New York and London, 1933.
- 10 T. Hirokawa and Y. Kiso, *J. Chromatogr.*, 260 (1983) in press.